

## Heat and Mass Transfer Hydromagnetic Radiative Casson Fluid Flow over an Exponentially Stretching Sheet with Heat Source/Sink

J. Prakash<sup>1</sup>, P. Durga Prasad<sup>2</sup>, G. Vinod Kumar<sup>3</sup>, R. V. M. S. S. Kiran Kumar<sup>4</sup>  
and S. V. K. Varma<sup>5</sup>

<sup>1</sup>Department of Mathematics, University of Botswana, Private Bag 0022, Gaborone, Botswana

<sup>2,3,4,5</sup>Department of Mathematics, S. V. University, Tirupati – 517502, A. P., India

Emails: [prakashj@mopipi.ub.bw](mailto:prakashj@mopipi.ub.bw)

[durga.prsd@gmail.com](mailto:durga.prsd@gmail.com); [gvkphd@gmail.com](mailto:gvkphd@gmail.com); [kksaisiva@gmail.com](mailto:kksaisiva@gmail.com); [svijayakumarvarma@yahoo.co.in](mailto:svijayakumarvarma@yahoo.co.in)

---

**ABSTRACT** :The present paper examines the hydromagnetic two-dimensional boundary layer flow of a non-Newtonian fluid accompanied by heat and mass transfer towards an exponentially stretching sheet in the presence of chemical reaction and thermal radiation. Casson model is used to characterize non-Newtonian fluid behavior. Using the similarity transformations, the governing partial differential equations are transformed into self-similar ordinary differential equations is solved by using Matlab bvp4c package. The effects of pertinent parameters are presented in both graphical and tabular form.

**KEYWORDS**- Casson fluid, chemical reaction, exponentially is stretching sheet, porous medium, thermal radiation.

---

### I. INTRODUCTION

The fluid flow behavior of non-Newtonian fluid has attracted special interest in recent years. The non-Newtonian fluids are mainly classified into three types, namely differential, rate, and integral. The simplest subclass of the rate type fluids is the Maxwell model which can predict the stress relaxation. This rheological model, also, excludes the complicated effects of shear-dependent viscosity from any boundary layer analysis was given by Hayat et al. [1]. In the category of non-Newtonian fluids, Casson fluid has distinct features. This model was presented by Casson for the flow of viscoelastic fluids in 1995. Casson fluid exhibits yield stress. It is well known that Casson fluid is a shear thinning liquid which is assumed to have an infinite viscosity at zero rate of shear, a yield stress below which no flow occurs, and a zero viscosity at an infinite rate of shear, i.e., if a shear stress less than the yield stress is applied to the fluid, it behaves like a solid, whereas if a shear stress greater than yield stress is applied, it starts to move. The examples of Casson fluid are of the type are as follows: jelly, tomato sauce, honey, soup, concentrated fruit juices, etc. Human blood can also be treated as Casson fluid. Fluids that belong to this category include cement, drilling mud, sludge, granular suspensions, slurries, paints, plastics, and paper pulp and food products. Due to the increasing importance of non-Newtonian fluids in industry, the stretching sheet concept has more recently been extended to fluids obeying non-Newtonian constitutive equations (Prasad et al. [2]). Khan [3] and Sanjayanand and Khan [4] have studied the viscous-elastic boundary layer flow and heat transfer due to an exponentially stretching sheet.

The MHD boundary layer flow of an incompressible and electrically conducting fluid is encountered in geophysics, astrophysics and in many engineering and industrial processes. The MHD heat and mass transfer flow in the boundary layer induced by a moving surface in a fluid finds important applications in electronics, meteorology, chemical engineering, and metallurgy etc. The study of boundary layer flow over continuous solid surface moving with constant velocity in an ambient fluid was initiated by Sakiadis [5]. Erickson et al. [6] extended Sakiadis [5] problem to include blowing or suction at the moving surface.

Convective heat transfer plays a vital role during the handling and processing of non-Newtonian fluid flows. Mechanics of non-Newtonian fluid flows present a special challenge to engineers, physicists, and mathematicians. Because of the complexity of these fluids, there is not a single constitutive equation which exhibits all properties of such non-Newtonian fluids. In the process, a number of non-Newtonian fluid models have been proposed. Amongst these, the fluids of viscoelastic type have received much attention. In the literature, the vast majority of non-Newtonian fluid are concerned of the types, e.g., like the power law and grade two or three (see Andersson and Dandapat [7], Hassanien [8], Sadeghy and Sharifi [9], Sajid et al. [10, 11]).

Mass transfer analysis in boundary layer flow is of great importance in extending the theory of separation processes and chemical kinetics (Bhattacharyya and Layek[12], [13], [14]). Andersson et al. [15] have discussed the transport of mass and momentum with chemical reactive species in the flow caused by a linear stretching sheet. Cortell [16] was analyzed mass transfer with chemically reactive species for two classes of viscoelastic fluid over a porous stretching sheet.

Diffusion of chemically reactive species in Casson fluid flow over a stretching surface was considered by Mukopadhyay [17, 18]. Nadeema [19] investigated an MHD boundary layer flow of Casson fluid over an exponentially permeable shrinking sheet. Casson fluid flow and heat transfer past an exponentially porous stretching surface in presence of thermal radiation was studied by Pramanik [20].

Inspired by the above investigations, in the present paper, the thermal and solutal boundary layer in incompressible, laminar flow over an exponentially stretching sheet with variable temperature and concentration in the presence of chemical reaction and thermal radiation is studied. The effect of pertinent parameters is presented in both graphical and tabular form.

## II. MATHEMATICAL FORMULATION

Consider the study two-dimensional MHD free convective laminar and incompressible viscous fluid past a flat sheet embedded in a porous medium moving with velocity  $U$ . Choose the coordinate system such that the  $y$  – axis is along the vertical direction and the  $x$  – axis normal to the plate. The physical model and coordinate system are shown in Fig.1. The plate is maintained at temperature  $T_w(x)$  and concentration  $C_w(x)$ . The temperature and the concentration of the ambient medium are assumed to be linearly stratified in the forms  $T_\infty(x) = T_{\infty,0} + A_1(x)$  and  $C_\infty(x) = C_{\infty,0} + B_1(x)$  respectively. Where  $A_1$  and  $B_1$  are constants and varied to alter the intensity of stratification in the medium,  $T_{\infty,0}$  and  $C_{\infty,0}$  are the beginning ambient temperature and concentration at  $x = 0$  respectively. The mass transfer phenomenon with chemical reaction is also retained. It is assumed that all body forces except magnetic field are neglected. A uniform magnetic field is applied normal to the direction of flow. The magnetic Reynolds number is assumed to be small so that the induced magnetic field can be neglected. The rheological equation of state for an isotropic and incompressible flow of a Casson fluid is as follows.

$$\tau_{ij} = \begin{cases} 2 \left( \mu_B + p_y / \sqrt{2\pi} \right) e_{ij}, & \pi > \pi_c \\ 2 \left( \mu_B + p_y / \sqrt{2\pi_c} \right) e_{ij}, & \pi < \pi_c \end{cases}$$

Here  $\pi = e_{ij} e_{ij}$  and  $e_{ij}$  is the  $(i, j)$ <sup>th</sup> component of the deformation rate,  $\pi$  is the product of the component of deformation rate with itself,  $p_y$  is the yield stress of the fluid,  $\mu_B$  is plastic dynamic viscosity of the non-Newtonian fluid,  $\pi_c$  is a critical value of this product based on non-Newtonian model. Let  $C_w$  be the concentration at the sheet and the concentration far away from the sheet is  $C_\infty$ .

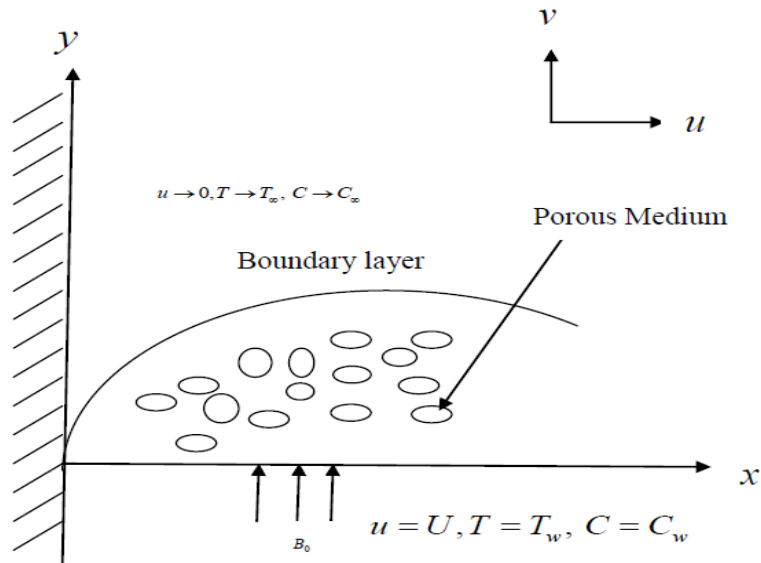


Fig 1. Sketch of the physical flow of problem

Under these assumptions along with the Boussinesq and boundary layer approximations, the system of equations, which models the flow is given by

$$\frac{\partial u}{\partial x} + \frac{\partial v}{\partial y} = 0, \quad (1)$$

$$u \frac{\partial u}{\partial x} + v \frac{\partial u}{\partial y} = \nu \left( 1 + \frac{1}{\beta} \right) \frac{\partial^2 u}{\partial y^2} - \frac{\sigma B_0^2 u}{\rho} - \frac{\nu}{K} u, \quad (2)$$

$$u \frac{\partial T}{\partial x} + v \frac{\partial T}{\partial y} = \alpha \frac{\partial^2 T}{\partial y^2} - \frac{1}{\rho C_p} \frac{\partial q_r}{\partial y} + \frac{Q}{\rho C_p} (T - T_\infty), \quad (3)$$

$$u \frac{\partial C}{\partial x} + v \frac{\partial C}{\partial y} = D \frac{\partial^2 C}{\partial y^2} - k (C - C_\infty), \quad (4)$$

where  $u$  and  $v$  are the velocity components along  $x$  and  $y$  -directions respectively,  $\nu$  is the kinematic viscosity,  $\alpha$  is the thermal diffusivity,  $\rho$  is the fluid density,  $\beta = \mu_B \sqrt{2\pi_c / p_y}$  is the Casson fluid parameter,  $D$  is the diffusion coefficient of the Casson fluid,  $K$  is the permeability of the fluid,  $Q$  is the dimensional heat source,  $q_r$  is the radiative heat flux, and  $C_p$  is the specific heat,  $k = k_0 e^{\frac{x}{L}}$  is the exponential reaction rate;  $k > 0$  stands for destructive reaction whereas  $k < 0$  stands for constructive reaction  $k_0$  is a constant.

The boundary conditions for the velocity, temperature and concentration fields are

$$u = U, v = 0, T = T_w, C = C_w \text{ at } y = 0, \quad (5)$$

$$u \rightarrow 0, T \rightarrow T_\infty, C \rightarrow C_\infty, \text{ as } y \rightarrow \infty \quad (6)$$

By using the Rosseland approximation, the radiative heat flux  $q_r$  was given by (Brewster [21])

$$q_r = \frac{4\sigma}{3K^*} \frac{\partial T^4}{\partial y}, \quad (7)$$

where  $\sigma$  is the Stefan-Boltzmann constant and  $K^*$  - the mean absorption coefficient. It should be noted that by using the Rosseland approximation, the present analysis is limited to optically thick fluids

$$T^4 \approx 4T_\infty^3 T - 3T_\infty^4, \quad (8)$$

$$\text{That is } q_r = \frac{4\sigma}{3K^*} \frac{\partial (4T_\infty^3 T - 3T_\infty^4)}{\partial y} = \frac{16T_\infty^3}{3K^*} \frac{\partial T}{\partial y}$$

In view of Eqns. (7) and (8), Eqn.(3) reduces to

$$u \frac{\partial T}{\partial x} + v \frac{\partial T}{\partial y} = \left( \alpha + \frac{16\sigma T_\infty^3}{3K^* \rho C_p} \right) \frac{\partial^2 T}{\partial y^2} + \frac{Q}{\rho C_p} (T - T_\infty), \quad (9)$$

Here  $U = U_0 e^{\frac{x}{2L}}$  is the stretching velocity (Magyari and Keller [22]),  $T = T_\infty + T_0 e^{\frac{x}{2L}}$  is the temperature and  $C_w = C_\infty + C_0 e^{\frac{x}{2L}}$  is the concentration at the sheet,  $U_0, T_0, C_0$  are the reference velocity, temperature and concentration respectively.

### III. METHOD OF SOLUTION

Introducing the similarity variables as

$$\eta = \sqrt{\frac{U_0}{2\nu L}} e^{\frac{x}{2L}} y, \quad u = U_0 e^{\frac{x}{2L}} f'(\eta), \quad v = -\sqrt{\frac{\nu U_0}{2L}} e^{\frac{x}{2L}} \left\{ f(\eta) + \eta f'(\eta) \right\},$$

$$T = T_\infty + T_0 e^{\frac{x}{2L}} \theta(\eta), \quad C = C_\infty + C_0 e^{\frac{x}{2L}} \phi(\eta), \quad B = B_0 e^{\frac{x}{2L}} \quad (10)$$

Substituting the similarity transformations (10) in equations (2) - (4) the governing equations reduce to

$$\left( 1 + \frac{1}{\beta} \right) f'''' + ff'' - 2f'^2 - \left( M + \frac{1}{K_p} \right) f' = 0, \quad (11)$$

$$\left( 1 + \frac{4R}{3} \right) \theta'' + \text{Pr} (f\theta' - f'\theta + S\theta) = 0, \quad (12)$$

$$\phi'' + Sc (f\phi' - f'\phi - 2\gamma\phi) = 0, \quad (13)$$

and the boundary conditions take the following form:

$$f' = 1, f = 0, \theta = 1, \phi = 1 \text{ at } \eta = 0 \quad (14)$$

$$f' \rightarrow 0, \theta \rightarrow 0, \phi \rightarrow 0 \text{ as } \eta \rightarrow \infty. \quad (15)$$

where the prime denotes differentiation with respect to  $\eta$ ,  $Sc = \frac{\nu}{D}$  is the Schmidt number,  $\text{Pr} = \frac{\nu}{\alpha}$  is the

Prandtl number,  $R = \frac{4\sigma T_\infty^3}{K^* K}$  is the Radiation parameter,  $S = \frac{Q}{2Lu\rho C_p}$  is the Heat source/sink parameter,

$M = \frac{\sigma B_0^2}{\mu B^2}$  is the magnetic field parameter,  $\frac{1}{K_p} = \frac{2L\nu}{u_0 C_p}$  is the Porous permeability parameter,  $\gamma = \frac{k_0 L}{U_0}$  is the

chemical reaction parameter. Here  $\gamma > 0$  represents the destructive reaction,  $\gamma = 0$  corresponds to no reaction, and  $\gamma < 0$  stands for the generative reaction.

Physical Quantities of Interest:

Local friction coefficient  $Cf$  is defined as

$$\frac{1}{\sqrt{2}} Cf \sqrt{R_e} = \left( 1 + \frac{1}{\beta} \right) f''(0) \quad (16)$$

The rate of heat and mass transfer coefficients at the plate are given by

$$q_w = -k \left( \frac{\partial T}{\partial y} \right)_{y=0}, \quad (17)$$

$$q_m = -D \left( \frac{\partial C}{\partial y} \right)_{y=0}, \quad (18)$$

$$\frac{Nu}{\sqrt{R_e}} = -\theta'(0), \quad (19)$$

$$\frac{Sh}{\sqrt{R_e}} = -\phi'(0), \quad (20)$$

$$\text{where } R_e = \frac{U_w}{\nu}. \quad (21)$$

#### IV. RESULTS AND DISCUSSION

The system of nonlinear ordinary differential equations (11) - (13) with the boundary conditions (14) and (15) are solved numerically by using bvp4c with MATLAB package. The abovementioned numerical scheme is carried out for various values of flow parameters, namely, the magnetic parameter ( $M$ ), the Casson parameter ( $\beta$ ), the Prandtl number (Pr), Heat source/sink parameter ( $S$ ), Porous permeability parameter ( $K_p$ ), Schmidt number (Sc), the thermal radiation parameter ( $R$ ) and Chemical reaction parameter ( $\gamma$ ) to obtain the effects of those parameters on dimensionless velocity, temperature and concentration distributions. The obtained computational results are presented graphically in Figs. 2–14 and the variations in velocity, temperature and concentration are discussed. Also, the Skin-friction factor, Nusselt number and Sherwood number are derived and given in tabular form.

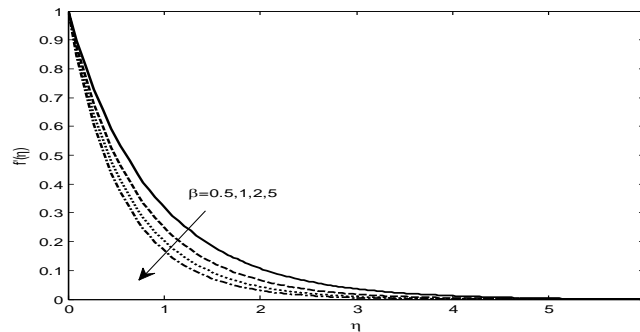


Fig.2 Variation of velocity  $f'(\eta)$  with  $\eta$  for several values of Casson parameter  $\beta$

$$Sc = 1, \gamma = 0.1, M = 0.5, K_p = 0.5, Pr = 1, R = 0.2, S = 0.1$$

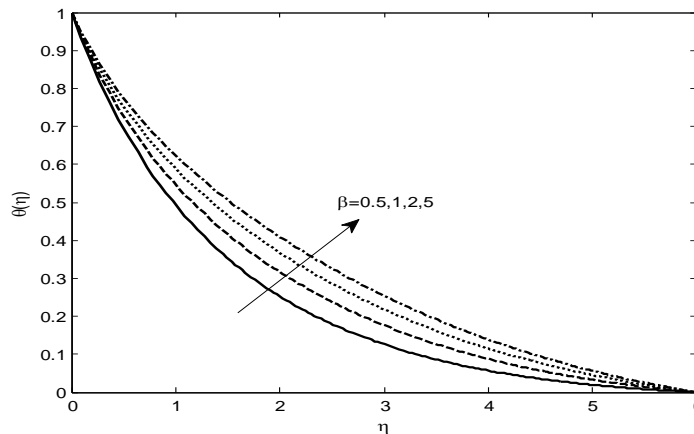


Fig.3 Variation of  $\theta(\eta)$  with  $\eta$  for several values of Casson parameter  $\beta$

$$Sc = 1, \gamma = 0.1, M = 0.5, K_p = 0.5, Pr = 1, R = 0.2, S = 0.1$$

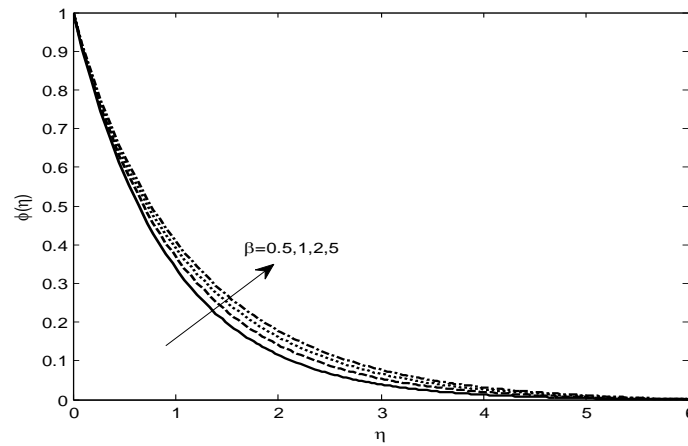


Fig.4 Variation of concentration  $\phi(\eta)$  with  $\eta$  for several values of Casson parameter  $\beta$

$$Sc = 1, \gamma = 0.1, M = 0.5, K_p = 0.5, Pr = 1, R = 0.2, S = 0.1$$

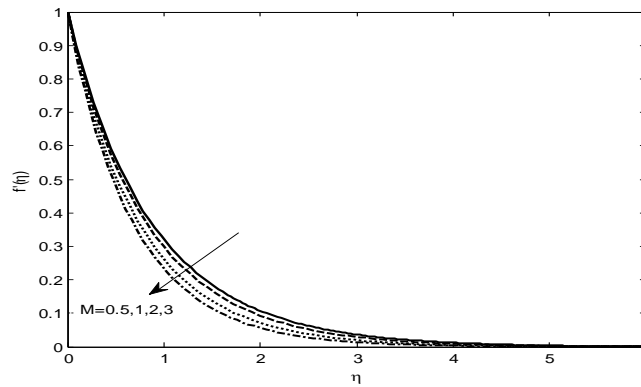


Fig.5 Variation of velocity  $f'(\eta)$  with  $\eta$  for several values of Magnetic parameter  $M$

$$Sc = 1, \gamma = 0.1, K_p = 0.5, Pr = 1, R = 0.2, S = 0.1, \beta = 0.5$$

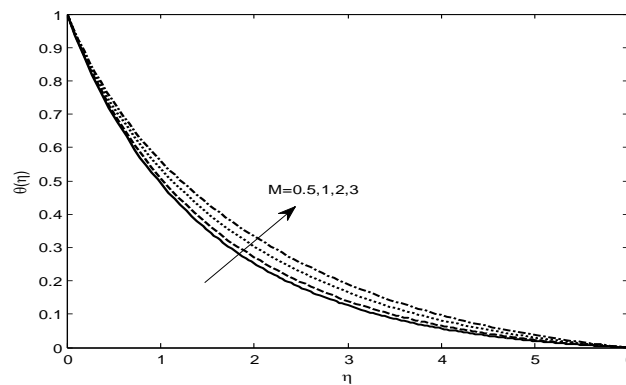


Fig.6 Variation of  $\theta(\eta)$  with  $\eta$  for several values of Magnetic parameter  $M$

$$Sc = 1, \gamma = 0.1, K_p = 0.5, Pr = 1, R = 0.2, S = 0.1, \beta = 0.5$$

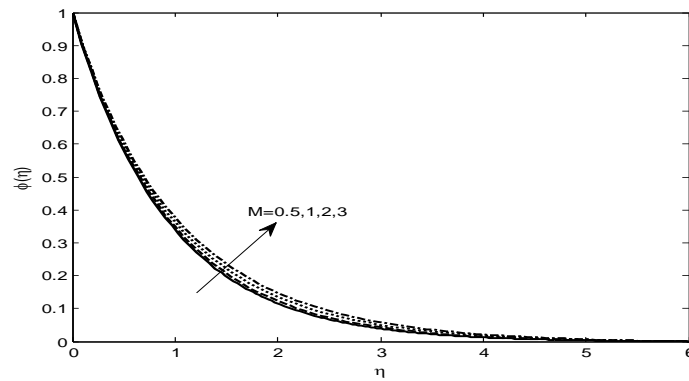


Fig.7 Variation of concentration  $\phi(\eta)$  with  $\eta$  for several values of Magnetic parameter  $M$

$$Sc = 1, \gamma = 0.1, K_p = 0.5, Pr = 1, R = 0.2, S = 0.1, \beta = 0.5$$

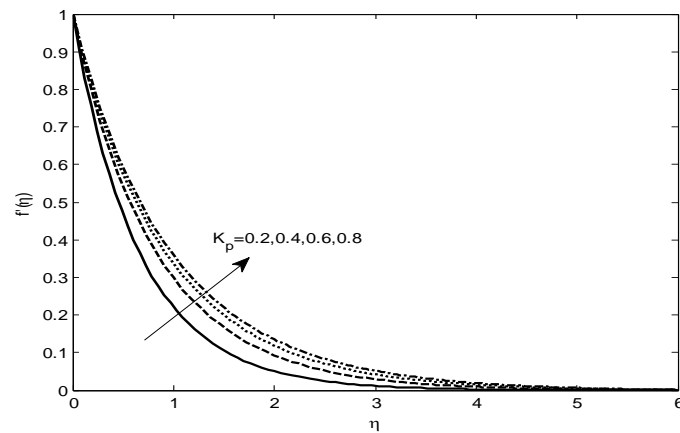


Fig.8 Variation of velocity  $f'(\eta)$  with  $\eta$  for several values of Porosity parameter  $K_p$

$$Sc = 1, \gamma = 0.1, Pr = 1, M = 0.5, R = 0.2, S = 0.1, \beta = 0.5$$

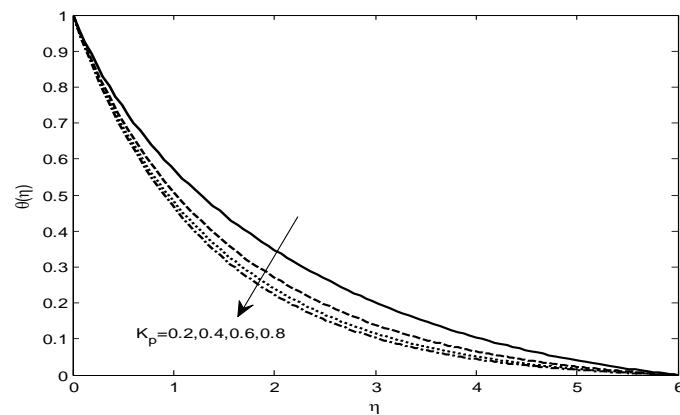


Fig.9 Variation of  $\theta(\eta)$  with  $\eta$  for several values of Porosity parameter  $K_p$

$$Sc = 1, \gamma = 0.1, Pr = 1, M = 0.5, R = 0.2, S = 0.1, \beta = 0.5$$

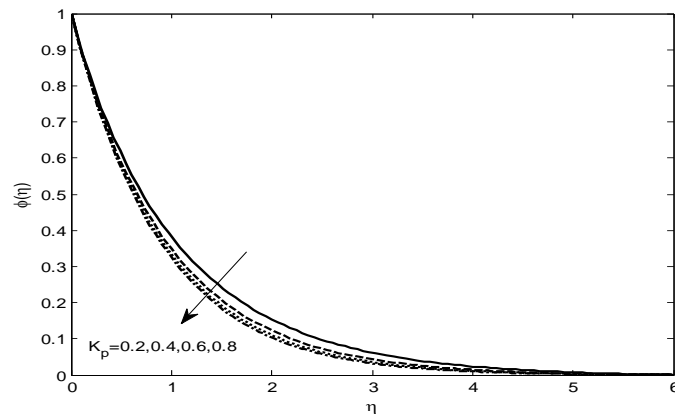


Fig.10 Variation of concentration  $\phi(\eta)$  with  $\eta$  for several values of Porosity parameter  $K_p$   
 $Sc = 1, \gamma = 0.1, Pr = 1, M = 0.5, R = 0.2, S = 0.1, \beta = 0.5$

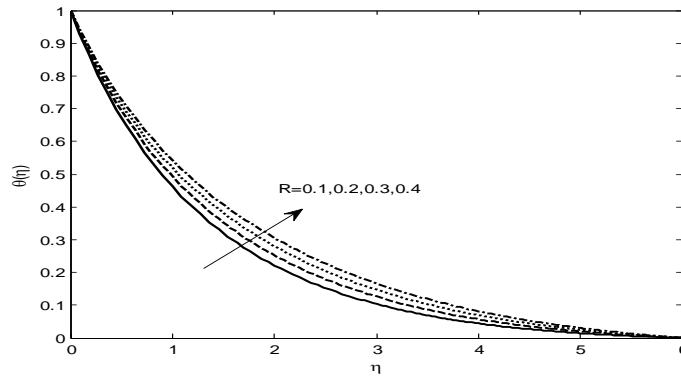


Fig.11 Variation of  $\theta(\eta)$  with  $\eta$  for several values of Radiation parameter R  
 $Sc = 1, K_p = 0.5, \beta = 0.5, M = 0.5, R = 0.2, S = 0.1, Pr = 1.$

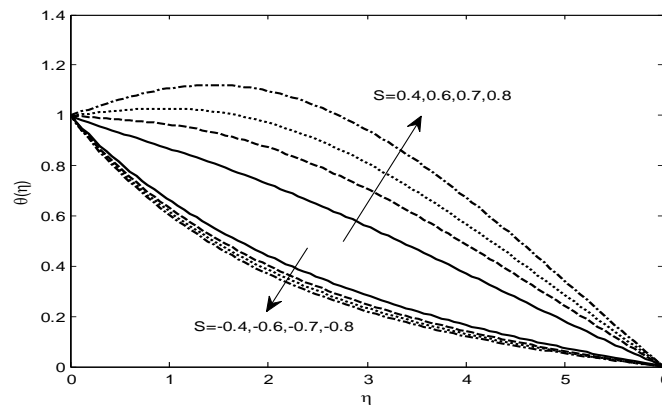


Fig.12 Variation of  $\theta(\eta)$  with  $\eta$  for several values of Heat Source/sink parameter S  
 $Sc = 0.60, Pr = 0.71, M = 2, R = 2, \gamma = 0.2, \beta = 0.5, K_p = 0.1$

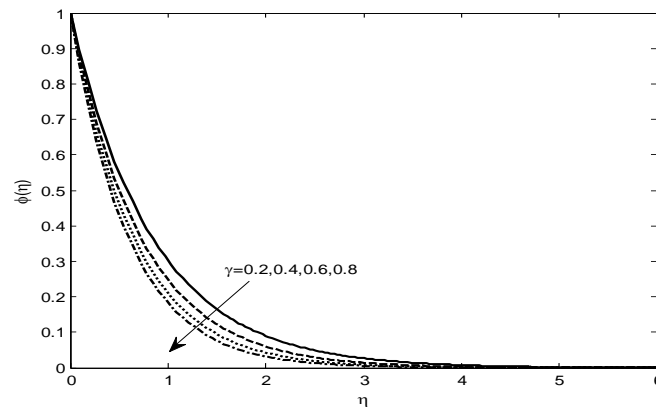


Fig.13 Variation of concentration  $\phi(\eta)$  with  $\eta$  for several values of Chemical reaction parameter  $\gamma$  with  $Sc = 1, Pr = 1, M = 0.5, R = 0.2, S = 0.1, \beta = 0.5, K_p = 0.5$

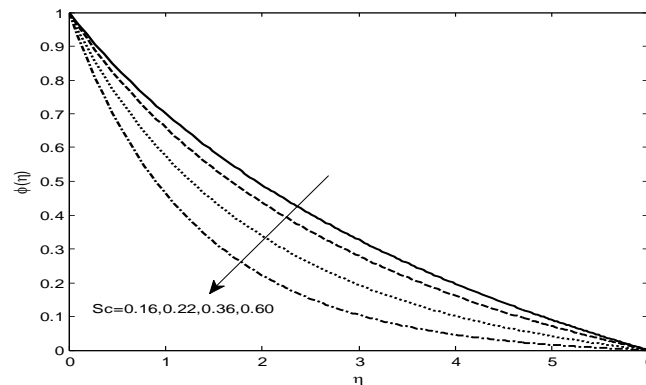


Fig.14 Variation of concentration  $\phi(\eta)$  with  $\eta$  for several values of Schmidt number  $Sc$   $\gamma = 0.1, K_p = 0.5, \beta = 0.5, M = 0.5, R = 0.2, S = 0.1, Pr = 1$ .

The velocity profiles for different values of Casson parameter  $\beta$  are depicted in Fig.2. The increasing values of the Casson parameter decreases yield stress and suppress the velocity field. The fluid behaves Newtonian fluid as Casson parameter becomes very large. From this figure it is also noticed that momentum boundary layer thickness decreases with an increase in Casson parameter. The temperature profiles for different values of Casson parameter  $\beta$  as shown in Fig.3. It is noticed that an increases in the temperature distribution along the thermal boundary layer is observed with a large enhancement in the Casson parameter as well as the thickness of thermal boundary layer increases. The nature of concentration profiles for various values of the Casson parameter is presented in Fig.4. It is observed that the species concentration increases with the increases in the Casson parameter  $\beta$ . Likewise, the solutal boundary layer thickness increases with increasing values of Casson parameters.

The dimensionless velocity and temperature profiles for various values magnetic parameter  $M$  is shown in Figs. 5, 6 and 7. It is observed that the thickness of momentum boundary layer decreases with increasing values of  $M$ . It is clear, because the increasing value of  $M$  tends to the increasing of Lorentz force, which produces more resistance to the transport phenomena, while the dimensionless temperature increases with  $M$ . The Lorentz force has the tendency to increase the temperature, and consequently, the thermal boundary layer thickness becomes thicker for stronger magnetic field it is shown in Fig.6. Similarly, from Fig.7 the solutal boundary layer thickness increases with the increasing values of  $M$ .

Figs. 8-10 display the effect of Porous permeability parameter on velocity, temperature and concentration profiles. Permeability is an important parameter for characterizing the transport properties, i.e. heat and mass transfer in porous medium. It is noticed that  $K_p$  increases the velocity, because increase in permeability of medium implies less resistance due to the porous matrix present in the medium while it decreases the temperature and concentration.

The effect of radiation parameter  $R$  on temperature field is shown in Fig.11. It is seen that thickness of the thermal boundary layer increases as  $R$  increases. It is clear that increase in the value of  $R$  implies increasing of thermal radiation in the thermal boundary layer which results in increase in the value of the temperature profile in the thermal boundary layer.

Fig.12 displays the variation of temperature profiles with respect to heat source and sink parameter  $S$ . It is noticed that the increase in heat source parameter increases the fluid temperature profile. It is seen that heat source can add more heat to the stretching sheet which increases its temperature. This increases the thickness of thermal boundary layer and the opposite trend is observed in the case of heat sink.

The effect of chemical reaction parameter  $\gamma$  on the concentration profiles is shown in Fig.13. It is observed that the concentration decreases with the increase of the chemical reaction i.e., the chemical reaction parameter decelerating agent and as a result, the solute boundary layer near the wall becomes thinner. This is due to fact that the conversion of the species takes place as a result of chemical reaction and thereby reduces the concentration in the boundary layer and hence increases the mass transfer.

The variation of the concentration profiles with the Schmidt number  $Sc$  is shown in Fig.14. As the Schmidt number  $Sc$  increases, the mass transfer rate increases. Actually the Schmidt number is inversely proportional to the diffusion coefficient  $D$ . Hence the concentration decreases with increasing  $Sc$ .

In order to verify the accuracy of the present results, we have considered the solutions obtained by [22], [23], [24], [25] and computed the numerical results for Nusselt number  $\theta'(0)$ . These computed results are tabulated in Table 1. It is interesting to observe from this table that the present results under some limiting conditions are in very good agreement with the computed results obtained from numerical solutions of [22], [23], [24], and [25]. Which clearly shows the correctness of the present results and computed results.

The numerical values of Skin friction coefficient ( $Cf$ ), Nusselt number ( $Nu$ ), and Sherwood number ( $Sh$ ) for different values of Magnetic field parameter ( $M$ ), Porous permeability parameter ( $K_p$ ) and Casson parameter ( $\beta$ ). It is observed from Table 2 that Nusselt number and Sherwood number decreases with increasing  $M$ , and  $\beta$ . But Skin friction coefficient is increases with  $M$ , and  $\beta$ , whereas the opposite trend is observed for Porous permeability parameter.

**Table1:** Comparison of the values of  $\theta'(0)$  for Radiation parameter  $R$ , Magnetic field parameter  $M$  and Prandtl number  $Pr$  for Newtonian fluid.

| R | M | Pr | Magyari and Keller [22] | El-Aziz [23] | Biddinand Nazar[24] | Ishak[25] | Present Results<br>( $R = 0, K_p = \infty, \beta = \infty$ ) |
|---|---|----|-------------------------|--------------|---------------------|-----------|--|
| 0 | 0 | 1  | -0.954782               | -0.954785    | -0.9548             | -0.9548   | -0.954813  |
| 0 | 0 | 2  | -                       | -            | -1.4714             | -1.4715   | -1.471457  |
| 0 | 0 | 3  | -1.869075               | -1.869074    | -1.8691             | -1.8691   | -1.869071  |
| 0 | 0 | 5  | -2.500135               | -2.500132    | -                   | -2.5001   | -2.500119  |
| 0 | 0 | 10 | -3.660379               | -3.660372    | -                   | -3.6604   | -3.660360  |
| 0 | 1 | 1  | -                       | -            | -                   | -0.8611   | -0.861508  |
| 1 | 0 | 1  | -                       | -            | -0.5315             | -         | -0.535302  |
| 1 | 1 | 1  | -                       | -            | -                   | -0.4505   | -0.461966  |

**Table 2:** Numerical values of Skin friction ( $Cf$ ), Nusselt number ( $Nu$ ), and Sherwood number

| $M$      | $K_p$      | $\beta$    | $-f''(0)$ | $-\theta'(0)$ | $-\phi'(0)$ |
|----------|------------|------------|-----------|---------------|-------------|
| <b>0</b> | 0.1        | 0.5        | 1.971819  | 0.202506      | 0.267806    |
| <b>1</b> | 0.1        | 0.5        | 2.054622  | 0.200714      | 0.265724    |
| <b>2</b> | 0.1        | 0.5        | 2.134212  | 0.199103      | 0.263847    |
| 0.5      | <b>0.2</b> | 0.5        | 1.545161  | 0.214151      | 0.281202    |
| 0.5      | <b>0.4</b> | 0.5        | 1.246353  | 0.225839      | 0.294411    |
| 0.5      | <b>0.6</b> | 0.5        | 1.129214  | 0.231616      | 0.300856    |
| 0.5      | 0.1        | <b>0.2</b> | 1.423863  | 0.217783      | 0.285351    |
| 0.5      | 0.1        | <b>0.4</b> | 1.864274  | 0.204930      | 0.270618    |
| 0.5      | 0.1        | <b>0.6</b> | 2.135795  | 0.199133      | 0.263880    |

## V. CONCLUSIONS

The numerical solutions for steady boundary layer heat and mass transfer flow of MHD Casson fluid over an exponentially permeable stretching surface in presence of first order chemical reaction, thermal radiation with heat source/sink are analyzed. The main findings of this investigation may be summarized as follows:

1. Momentum boundary layer thickness decreases with increasing Casson parameter but the thermal and solutal boundary layer thickness increases in this case.
2. The temperature increases with increasing values of the radiation parameter. This phenomenon is ascribed to a higher effective thermal diffusivity.
3. The solutal boundary layer thickness decreases with increasing values of destructive chemical reaction parameter and Schmidt number.
4. It is observed that the increase in magnetic field parameter enhanced the skin friction coefficient. The magnetic field creates Lorentz force which increases the value of skin friction coefficient. But the reverse effect is seen in case of porosity parameter.
5. The Casson parameter increases the skin friction coefficient. However, the velocity is decreased when the Casson parameter is increased. Moreover, Nusselt number and Sherwood number is decreases.

## REFERENCES

- [1] T. Hayat, M. Awais, M. Sajid, Mass transfer effects on the unsteady flow of UCM fluid over a stretching sheet. *Int J Mod Phys B*. 25, (2011) 2863–2878.
- [2] K.V. Prasad, S. Abel, P.S. Datti, Diffusion of chemically reactive species of a non-Newtonian fluid immersed in a porous medium over a stretching sheet. *Int. J. of Non-Linear Mech.*38, (2003) 651 – 657.
- [3] S.K. Khan, Boundary layer viscoelastic fluid flow over an exponentially stretching sheet, *Int. J. of Appl. Mech. and Engng.*11, (2006) 321-335.
- [4] E. Sanjayanand, S. K. Khan, on heat and mass transfer in a visco-elastic boundary layer flow over an exponentially stretching sheet, *Int. J. of Ther. Sci.*, 45, (2006) 819-828.
- [5] B.C. Sakkiadis, Boundary layer behaviours on continuous surface. *AIChE.*7, (1961) 221- 225.
- [6] L. E. Erickson, L. T. Fan, V. G. Fox, Heat and mass transfer on a moving continuous plate with suction and injection. *Ind. Eng. Chem. Fundamental.*5, (1966) 19-25.
- [7] H. I. Andersson, B. S. Dandapat, Flow of a power law fluid over a stretching sheet. *Appl. Anal. Continuous Media.*1,(1992) 339–347.
- [8] I. A. Hassanien, Flow and heat transfer on a continuous flat surface moving in a parallel free stream of power-law fluid. *Appl. Model.* 20,(1996) 779–784.
- [9] K. Sadeghy, M. Sharifi, Local similarity solution for the flow of a 'second-grade' viscoelastic fluid above a moving plate. *Int J Nonlinear Mech.* 39, (2004) 1265–1273.
- [10] M. Sajid, T. Hayat, S. Asghar, Non-similar analytic solution for MHD flow and heat transfer in a third-order fluid over a stretching sheet. *Int. J Heat Mass Transfer.*50, (2007) 1723–1736.
- [11] M. Sajid, I. Ahmad, T. Hayat, M. Ayub. Unsteady flow and heat transfer of a second grade fluid over a stretching sheet. *Commun Nonlinear ScisNumSimul.* 14, (2009) 96–108.
- [12] K. Bhattacharyya, and G.C. Layek, Chemically reactive solute distribution in MHD boundary layer flow over a permeable stretching sheet with suction or blowing, *Chem. Eng. Commun.*, 197,(2010) 1527–1540.
- [13] K. Bhattacharyya, Boundary layer flow and heat transfer over an exponentially shrinking sheet, *Chin. Phys. Lett.* 28, (2011) 1-4.

- [14] K. Bhattacharyya, and G.C. Layek, Similarity solution of MHD boundary layer flow with diffusion and chemical reaction over a porous flat plate with suction/blowing, *Meccanica*, 47, (2012) 1043–1048.
- [15] H. I. Andersson, O. R. Hansen, and B. Holmedal, Diffusion of a chemically reactive species from a stretching sheet, *Int. J. Heat Mass Transfer*. 37, (1994) 659–664.
- [16] R. Cortell, Toward an understanding of the motion and mass transfer with chemically reactive species for two classes of viscoelastic fluid over a porous stretching sheet, *Chem. Eng. Process.*, 46, (2007) 982–989.
- [17] S. Mukhopadhyay and G. Rama Subba Reddy, Diffusion of chemically reactive species of a Casson fluid flow over an exponentially stretching surface. *J. Thermal Energy and Power Engineering*. 3, (2014) 216-221.
- [18] S. Mukhopadhyay, K. Vajravelu, Diffusion of chemically reactive species in Casson fluid flow over an unsteady permeable stretching surface. *J. Hydrodynamics, Ser. B*.25, (2013) 591–598.
- [19] S. Nadeema, RizwanUlHaq, C. Lee, MHD flow of a Casson fluid over an exponentially shrinking sheet. *ScientiaIranica B*.19, (2012) 1550–1553.
- [20] S. Pramanik, Casson fluid flow and heat transfer past an exponentially porous stretching surface in presence of thermal radiation. *Ain Shams Engineering Journal*. 5, (2014) 205–212.
- [21] M. Q. Brewster, *Thermal radiative transfer properties*. John Wiley and Sons; 1972.
- [22] E. Magyari, B. Keller, Heat and mass transfer in the boundary layers on an exponentially stretching continuous surface. *J. Phy. D. Appl. Phy.* 32, (1999) 577-585.
- [23] M A. El-Aziz, Viscous dissipation effect on mixed convection flow of a micropolar fluid over an exponentially stretching sheet. *Can. J. Phys.* 87, (2009) 359-368.
- [24] B. Bidin, R. Nazar, Numerical solution of the boundary layer flow over an exponentially stretching sheet with thermal radiation. *Euro.J.of Sci. Resc.*33, (2009) 710-717.
- [25] A. Ishak, MHD boundary layer flow due to an exponentially stretching sheet with radiation effect. *Sains Malaysiana*, 40, (2011) 391-395.